



Seasonal measurements of the nitrogenous osmolyte glycine betaine in marine temperate coastal waters

Ruth L. Airs · Rachael Beale · Luca Polimene · Yin Chen · Michaela A. Mausz · David J. Scanlan · Claire E. Widdicombe · Glen A. Tarran · E. Malcolm S. Woodward · Carolyn Harris · Andrea McEvoy

Received: 23 August 2022 / Accepted: 5 December 2022
© The Author(s) 2022

Abstract Glycine betaine (GBT) is a nitrogenous osmolyte ubiquitous throughout the marine environment. Despite its widespread occurrence and significance in microbial cycling, knowledge of the seasonality of this compound is lacking. Here, we present a seasonal dataset of GBT concentrations in marine suspended particulate material. Analysing coastal waters in the Western English Channel, GBT peaked in summer and autumn but did not follow the observed maxima in total phytoplankton biomass or

chlorophyll *a*. Instead, we found evidence that GBT concentrations were associated with specific phytoplankton groups or species, particularly in the summer when GBT correlated with dinoflagellate biomass. In contrast, autumn maxima corresponded with a period of rapidly changing salinity and nutrient availability, with potential contributions from some phytoplankton species and Harpacticoid copepods. This suggests distinct environmental drivers for different periods of the GBT seasonality. Building on evidence that GBT and dinoflagellate biomass peak in summer, concomitantly with low nutrients, we propose that GBT positively affects dinoflagellate fitness, allowing them to outcompete other plankton when inorganic nutrients are depleted. By using

Responsible editor: Francis Chan.

Supplementary Information The online version contains supplementary material available at <https://doi.org/10.1007/s10533-022-01006-7>.

R. L. Airs (✉) · R. Beale · L. Polimene · C. E. Widdicombe · G. A. Tarran · E. M. S. Woodward · C. Harris · A. McEvoy
Plymouth Marine Laboratory, Prospect Place, Plymouth, Devon PL1 3DH, UK
e-mail: ruai@pml.ac.uk

R. Beale
e-mail: rbea@pml.ac.uk

L. Polimene
e-mail: L.polimene@gmail.com

C. E. Widdicombe
e-mail: CLST@pml.ac.uk

G. A. Tarran
e-mail: gat@pml.ac.uk

E. M. S. Woodward
e-mail: emsw@pml.ac.uk

C. Harris
e-mail: caha@pml.ac.uk

A. McEvoy
e-mail: ajmc@pml.ac.uk

Y. Chen · M. A. Mausz · D. J. Scanlan
School of Life Sciences, Gibbet Hill Campus, University of Warwick, Coventry, Warwickshire CV4 7AL, UK
e-mail: Y.Chen.25@warwick.ac.uk

M. A. Mausz
e-mail: M.Mausz@warwick.ac.uk

D. J. Scanlan
e-mail: D.J.Scanlan@warwick.ac.uk

this assumption, we improved the performance of a marine ecosystem model to reproduce the observed increase in dinoflagellates biomass in the transition from spring to summer. This work sheds light on the interplay between phytoplankton succession, competitive advantage and changing environmental factors relevant to climate change. It paves the way for future multidisciplinary research aiming to understand the importance of dinoflagellates in key coastal ecosystems and their potential significance for methylamine production, compounds relevant for particle growth in atmospheric chemistry.

Keywords Glycine betaine · Osmolytes · Phytoplankton · Marine · Dinoflagellates · Western Channel Observatory

Introduction

Glycine betaine (GBT) is a zwitterionic, nitrogen containing cellular osmolyte widely used in the marine environment by bacteria and phytoplankton. The biosynthetic pathways of GBT in some species of phytoplankton have been partly elucidated (Kageyama et al. 2018). GBT transporters are found frequently in marine bacterial genomes and its transcripts can be readily detectable in metatranscriptomics datasets (McParland et al. 2021). Further, once glycine betaine is taken up by marine microbial communities, a high proportion remains unmetabolized (Kiene and Hoffman-Williams 1998; Boysen et al. 2022), indicating this compound's importance in osmotic function. The metabolism of glycine betaine appears quite specialised (McParland et al. 2021), but this compound is also widely used—labelled nitrogen from GBT made its way through the entire microbial community (Boysen et al. 2022). Further, a recent study looking at seasonal microbial uptake of glycine betaine showed evidence for a wider capacity for GBT catabolism than previously realised (Mausz et al. 2022). The highly abundant SAR11 bacterioplankton of the Alphaproteobacteria clade has high affinity transporters and can use GBT as an energy source and fuel the C1 cycle (Noell and Giovannoni 2019). In culture, model organisms of the abundant marine Roseobacter clade can grow on GBT as a sole carbon source (Lidbury et al. 2015) resulting in remineralisation of the osmolyte nitrogen to ammonia

(Zecher et al. 2020), thereby making the nitrogen available to a plethora of microorganisms, partly explaining the value of this compound to the marine microbial community. Marine methanogens can also grow on glycine betaine (King 1984; Watkins et al. 2014), and glycine betaine can degrade aerobically to methane, linking to biological methane production. Furthermore, glycine betaine can degrade anaerobically to form methylamines (Heijthuijsen et al. 1989), providing a marine biogenic source of atmospheric amines (Dall'Osto et al. 2017,2019), thought to be relevant for the important climate processes of new particle formation and growth (Almeida et al. 2013; Riccobono et al. 2014).

Despite the importance of glycine betaine to the microbial community and as a precursor to climate active methylamines, field measurements of GBT are still relatively uncommon. The application of metabolomics studies to marine metabolites (e.g. Boysen et al. 2018) has revealed strong diel cycling of osmolytes (Boysen et al. 2021), indicating rapid cycling in the environment and much wider use than osmotic function. Investigation of suspended and sinking metabolites has shown the dominance of glycine betaine and proline with depth (Johnson et al. 2020), likely driven by the microbial communities associated with sinking particles. Targeted analyses for osmolytes reveal higher concentrations in ice influenced regions of Antarctic waters (Dall'Osto et al. 2017, 2019) and higher concentrations in coastal regions compared to the open ocean (Airs and Archer 2010; Keller et al. 2004; Beale and Airs 2016). Recently, Sacks et al. (2022) developed a method to determine a wide range of metabolites from the dissolved phase, including GBT, in marine and freshwater samples. Nevertheless, this limited knowledge has come from only a handful of studies or data points.

Phytoplankton culture studies have shown that of 15 phytoplankton species tested, five produced GBT at a higher concentration than the sulphur osmolyte dimethylsulphoniopropionate (DMSP; in four species DMSP was not detected at all, Spielmeier et al. 2011), suggesting global production of GBT to be significant compared to DMSP, which is estimated at 2 petagrams (2×10^9 tons) of sulphur in the upper ocean, annually (Galí et al. 2015). Other physiological functions of GBT include acting as a chemoattractant in the marine microbial food web (Seymour et al. 2010), accelerating the recovery of

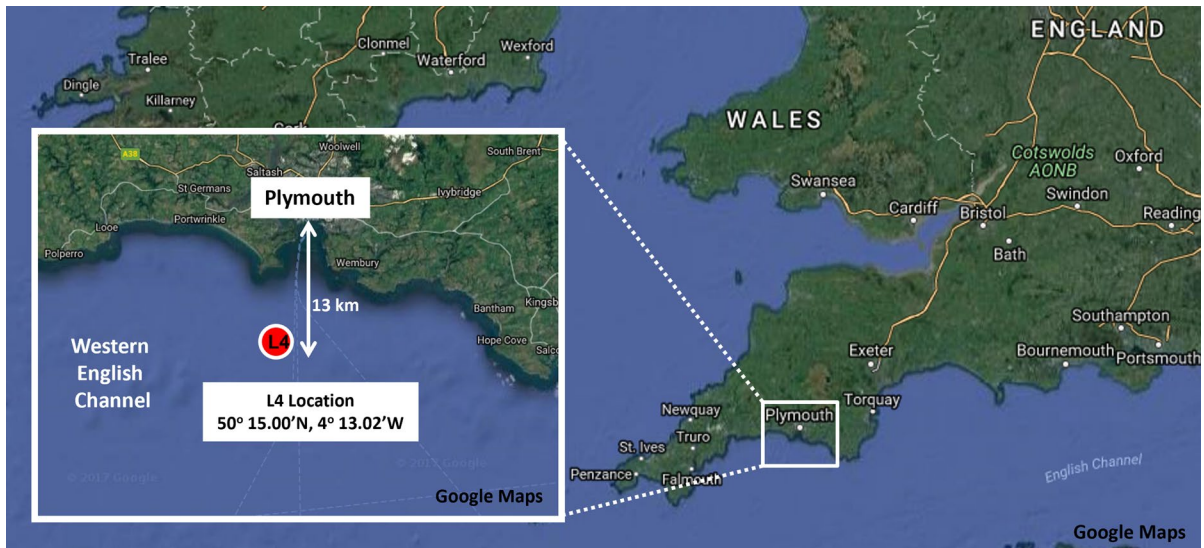


Fig. 1 Position of Station L4, 13 km off the Plymouth Coast, in the Western English Channel, UK. Figure produced using Google Maps and www.latlong.net

photosystem II from high light exposure (Papageorgiou and Murata 1995; Kondo et al. 1999; Prasad and Saradhi 2004) and as a cryoprotectant in sea ice algae (Thomas and Dieckmann 2002).

Despite the importance of glycine betaine as an osmolyte, as a precursor for climate active compounds and as an important component in microbial C, N and energy flow, there is relatively little information about osmolyte distributions in the marine environment, especially not any reported seasonal data; and we know little about the conditions that control intracellular osmolyte concentrations. Here, we provide a comprehensive dataset of the first seasonality of particulate GBT abundance in surface waters sampled at a coastal observatory in the Western English Channel (Fig. 1).

Measurements are presented in the context of phytoplankton species biomass and succession, temperature, salinity and other biological and physicochemical parameters. The data has led to the hypothesis that GBT production enhances the growth of dinoflagellates under nutrient depleted conditions, allowing them to dominate the phytoplankton community in the summer season, and this hypothesis was tested by developing a mathematical formulation describing GBT dynamics and implementing it in a marine ecosystem model.

Materials and methods

Sampling site

Station L4 is a coastal station located in the Western English Channel ($50^{\circ} 15.00' N$, $4^{\circ} 13.02' W$), approximately 13 km off the Plymouth coast (Fig. 1). The RV *Plymouth Quest* samples Station L4 weekly (weather permitting), as part of the on-going and long-term Western Channel Observatory (www.westernchannelobservatory.org.uk). Various physical, chemical and biological measurements have been recorded at Station L4 since 1988 (Smyth et al. 2010).

Collection of particulate samples for determination of glycine betaine (GBT) began in March 2016 and continued until December 2016. Water was collected via a conductivity, temperature and depth (CTD) profiler with individually sprung 10 L Niskin bottles. Water for GBT was collected from the 'surface' Niskin bottle, typically from a depth of 2 m and was immediately transferred into a 10 L vessel via Tygon tubing. During the return trip to the laboratory samples were maintained at sea surface temperature (via flushing the outside of the container with surface water) in the dark. Sample preparation, extraction and analysis commenced immediately upon arrival back at the laboratory, typically within 2–3 h of collection.

Quantitation of GBT

The methodology for the determination of particulate N-osmolytes has been recently published (Beale and Airs 2016) so only a brief description is provided here. Glycine betaine (GBT) reference standard was supplied by Sigma Aldrich. A deuterated internal standard (d_{11} -GBT) (Cambridge Isotope Laboratories Inc.) was added to both standards and samples.

Seawater (approx. 4 L) was first passed through a 200 μm mesh into a large beaker to exclude zooplankton. Small volume aliquots of 2 mL were then taken from this reservoir using a syringe and filtered through polycarbonate (PC) filters (47 mm diameter, 0.2 μm pore size, supplied by Fisher Scientific), held within a Swinnex filter holder (Millipore). A small volume was chosen for filtration because during filtration of large volumes, loss of particulate analytes from cells to the dissolved phase has been shown previously (Fuhrman and Bell 1985). Kiene and Slezak (2006) advised filtering no more than 3.5 mL to preserve cell structure when collecting dissolved phase samples for DMSP analysis. As GBT has also been shown to be susceptible to the manner of particulate collection (Airs and Archer 2010); a sample volume of 2 mL was chosen and triplicate samples were taken. Neither vacuum nor gravity filtration were employed which reduced the risk of cell disruption. Instead, an in-line filter was used, reducing the time the sample was in contact with laboratory air (Beale and Airs 2016). Filters were pre-rinsed in 100% methanol (LC/MS grade, Fisher Scientific) to remove contaminants (Beale and Airs 2016).

Following filtration, the underside of the filter was blotted on glass fibre filter paper (GF/F, Fisher Scientific) to remove excess seawater which has been shown to cause ion suppression during analysis (Beale and Airs 2016). The filter was immersed in 1.5 mL extraction solvent (methanol:chloroform:water at a ratio of 12:5:1) (chloroform HPLC grade, VWR) in an extraction tube (50 mL, Sarstedt). Internal standard (d_{11} -GBT) was then added (10 μL) to the extraction tube to generate a concentration of 10 $\text{pg } \mu\text{L}^{-1}$ (equivalent to 200 pg per 20 μL injection). After a brief vortex, the filter was left to soak for 1 h. Following extraction, the solvent was transferred with a Pasteur pipette (VWR) to a 2 mL Eppendorf tube (Sigma Aldrich) for centrifugation (4 min at $9447\times g$). The

supernatant was then transferred into an HPLC vial (Kinesis) for analysis.

Quantification of GBT was achieved using liquid chromatography/mass spectrometry comprising an Agilent 1200 High Pressure Liquid Chromatograph (HPLC) and a 6330 Ion Trap Mass Spectrometer (MS) with Electrospray Ionisation (ESI). A binary mobile phase was used: 0.15% formic acid + 10 mM ammonium acetate (A) and 100% methanol (LC/MS-grade) (B) in an isocratic run at a ratio of 80:20 A:B. The injection volume was 20 μL into a mobile phase flow of 0.35 mL min^{-1} . An HSF5 Discovery column (15 cm \times 2.1 mm, 3 μm) and associated guard column (2 cm \times 2.1 mm, 3 μm , both Supelco) were used at a temperature of 60 $^{\circ}\text{C}$ for separation of compounds before identification via mass spectrometry. Electrospray source settings were as follows; positive ion mode, nebuliser gas at 55 psi, drying gas at 12 L min^{-1} , vaporiser temperature at 350 $^{\circ}\text{C}$. The resulting ionised compounds were detected at m/z 129 (d_{11} -GBT) and 118 (GBT).

Calibration was performed on each day of sample analysis and consisted of standards (typically $n=7$; prepared in extraction solvent, see above) containing increasing amounts of GBT to span *in-situ* sample concentrations. Deuterated internal standard was spiked at a consistent concentration into all standards and samples (10 $\text{pg } \mu\text{L}^{-1}$). Check standards prepared at a single concentration were analysed every 3 samples during the sequence to monitor instrument response throughout the entire run. Peak area ratios were calculated for both standards and samples by dividing analyte peak area by the internal standard peak area. Calculation of concentration was achieved by direct comparison of the sample peak area ratio to that of the standard calibration. Limits of detection (LOD) for the method were calculated to be 1.5 nmol L^{-1} for GBT (Beale and Airs 2016).

Analysis of environmental parameters at Station L4

Ancillary data were collected at L4 over the same period. Chlorophyll *a* was determined by Turner fluorometry according to Welshmeyer (1994). Nutrient concentrations including nitrate and nitrite were analysed according to Woodward and Rees (2001) using a segmented flow colorimetric nutrient auto-analyzer (SEAL). Phytoplankton species were determined using light microscopy for selected dates that

coincided with GBT sampling. Paired 200 mL samples were collected from 10 m depth, with one preserved with acid Lugol's iodine and the other neutral formaldehyde. A 50 mL and 100 mL subsample of the Lugol's and formaldehyde-preserved samples, respectively, were analysed by light microscopy using the Utermöhl settling technique to enumerate phytoplankton > 2 µm including diatoms, dinoflagellates, coccolithophores, *Phaeocystis*, ciliates and flagellates (Widdicombe et al. 2010). Individual cells were identified to species level, where possible. Taxa-specific cell biovolumes were converted to biomass using the equations of Menden-Deuer and Lessard (2000). For zooplankton sampling and analysis, paired samples were collected weekly by vertical hauls of a WP2 net (57 cm diameter, mesh 200 µm) from 50 m to the surface and stored in 4% formalin. Zooplankton were identified and enumerated using light microscopy. Taxonomy of both phytoplankton and zooplankton is based on the World Register of Marine Species (WORMS) scheme and further information is available at https://www.westernchannelobservatory.org.uk/l4_zooplankton.php. Autonomous CTD-mounted sensors recorded temperature, salinity and photosynthetically active radiation data.

Ecosystem modelling

Model simulations were performed by using the European Regional Seas Ecosystem Model (ERSEM) fully described in Butenschön et al. (2016). ERSEM is a biomass and functional types-based biogeochemical model describing the cycling of carbon and nutrients (N, P and Si) in the pelagic and benthic environment. One of the main features of this model is that the carbon to nutrient ratios (C:N:P) are not constant but are instead variable depending on the environmental nutrient conditions. Each functional type is therefore described through variable carbon, nitrogen, phosphorus and (only for diatoms) silica concentrations. For this specific feature, ERSEM has been successfully used to simulate nutrient stress-driven dynamics (e.g. Pinna et al. 2015, Polimene et al. 2012). Primary producers are represented by 4 functional types describing diatoms (P1), nanophytoplankton (P2), picophytoplankton (P3) and microphytoplankton (P4). In this work we focussed on the functional type P4 which for its specific features such as slow growth rate, low chlorophyll content

and relatively low grazing pressure upon it, has been traditionally used to simulate dinoflagellates (Pinna et al. 2015, Torres et al. 2020). The formulation of this functional type (hereafter dinoflagellates) was modified by including a new formulation describing GBT cellular production and its effect on cell fitness according to our working hypothesis. The new model formulation is described below. ERSEM was coupled with the General Ocean Turbulence Model (GOTM, Burchard et al. 1999) and implemented at L4 as in Butenschön et al. (2016). The model was run for 7 years (2010–2016). The simulations presented in the paper refer to 2016, when the GBT measurements were performed.

GBT production, loss and its effect on dinoflagellate physiology

GBT dynamics are described mirroring the formulation used in Pinna et al. (2015) for the production of toxins in dinoflagellates. According to this, GBT concentration ($\mu\text{mol m}^{-3}$) was described through the following equation:

$$\frac{\partial \text{GBT}}{\partial t} = \text{GBT}_{\min} \cdot \text{NPP} + \phi \cdot \left(1 - \frac{\text{GBT}_C}{\text{GBT}_{\max}}\right) \cdot \text{Lim} \cdot C - \text{Loss} \quad (1)$$

Where GBT_{\min} is the minimal GBT cellular quota (given as GBT:C ratio) produced as a fixed fraction of the net primary production (NPP), GBT_{\max} is the maxima quota achievable under nutrient limitation and GBT_C is the actual GBT to carbon ratio. The parameter ϕ represents the fraction of carbon daily invested into GBT production under nutrient limitation, while C is the biomass given as carbon concentration (mg m^{-3}). The function *Lim* is given by:

$$\text{Lim} = \max\left(0, 1 - \frac{\text{nutlim}}{sc}\right) \quad (2)$$

Where *nutlim* is the function describing nutrient limitation in ERSEM and *sc* is a scaling factor meant to regulate the internal nutrient quota at which enhanced production of GBT starts. The value of *Lim* as a function of the internal nutrient quota is given in supplementary Fig. 2. It should be noted here that GBT synthesis is assumed to be supported by the reallocation of cellular resources i.e. without additional metabolic costs (respiration). Enhanced production of GBT is mirrored by the down regulation of chlorophyll

Table 1 GBT model parameters

Parameter	Unit	Value
GBT_{min} (min GBT to C ratio)	$[\mu\text{mol (GBT) (mg C)}^{-1}]$	0.2
GBT_{max} (max GBT to C ratio)	$[\mu\text{mol (GBT) (mg C)}^{-1}]$	1.5
ϕ (Daily GBT production relative to carbon under nutrient limitation)	$[\mu\text{mol (GBT) (mg C)}^{-1} \text{d}^{-1}]$	1.0
SC (Scaling factor)	Adimensional	0.6

a under nutrient stress conditions which is already described in the model (Butenschön et al. 2016, Pinna et al. 2015). This implies that GBT synthesis is performed at the “cost” of reduced photosynthetic capacity.

GBT loss (*Loss*) is modelled by scaling carbon loss terms already described in ERSEM by the actual GBT:C ratio:

$$Loss = (mortality + restrespiration + grazing) \cdot GBT_C \quad (3)$$

In order to test the hypothesis that increasing cellular GBT gives a competitive advantage to dinoflagellates, we have assumed that mortality (M), respiration

(R) and cell sinking rate (S) linearly decrease as soon as GBT_C exceeds GBT_{min} :

$$F_{M,R,S}^* = F_{M,R,S} \cdot \frac{GBT_{min}}{GBT_C} \quad (4)$$

where F_i^* ($i = M, R, S$) are the actual mortality, respiration and sinking rate fluxes and F_i ($i = M, R, S$) are the same fluxes as described in ERSEM (Butenschön et al. 2016).

Model parameters relative to the new GBT formulation (Table 1) were manually tuned to obtain the simulations shown in Fig. 2 and summarised in Table 2.

Results and discussion

Site description

Station L4 of the Western Channel Observatory is a temperate coastal site which experiences seasonal stratification and riverine influences due to its proximity to the Plymouth coast and the mouth of the River Tamar (Fig. 1). Nutrient concentrations (Nitrate+Nitrite, Fig. 3c) in 2016 were typical of this coastal station (Smyth et al. 2010), with a decrease in nutrients in spring due to rapid depletion by phytoplankton, low levels throughout summer, and replenishment in autumn once thermal stratification breaks down. Sea surface temperature

Table 2 Observed and simulated seasonal mean values of GBT and percentage of dinoflagellates with respect to the total phytoplankton biomass (sd); [min-max]. Spring/Summer defined as in Fig. 3

	Spring		Summer	
	GBT (nmol L ⁻¹)	Dino%	GBT (nmol L ⁻¹)	Dino%
Data	5.1 (2.2) [1.2–8.7]	16 (10) [3–33]	28.5 (18.8) [12.8–68.3]	81 (9) [65–92]
ERSEM+GBT	2.6	11	21.2	38
ERSEM		8		10

Fig. 2 Observed and modelled GBT concentrations. Data are displayed with standard deviation

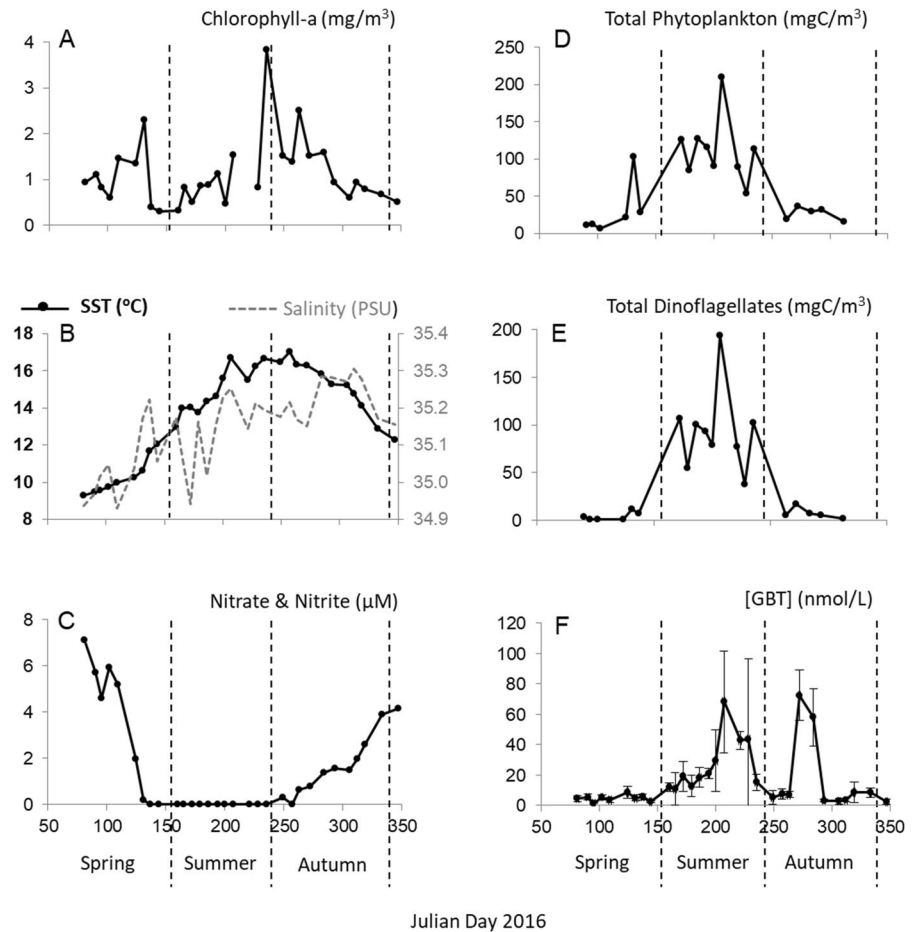


(Fig. 3b) increased from May to reach a maximum of 17 °C in September. Surface salinity at L4 during 2016 (Fig. 3b) was lowest during spring with surface freshening typically attributed to increased precipitation and pulses of freshwater from the River Tamar (Smyth et al. 2010). The seasonality of physicochemical variables at L4 leads to phytoplankton succession, with a relatively stable community in winter, and an abrupt change in diversity and biomass in spring, with increased abundance of several phytoplankton groups in April, including diatoms, *Phaeocystis* and Coccolithophorids (Widdicombe et al. 2010). In summer, the composition is typically varied, before returning to winter composition in October (Widdicombe et al. 2010). During the period of study, chlorophyll *a* peaked in spring and again in late summer and remained elevated until mid-autumn (Fig. 3a). Phytoplankton counts to species level were performed on twenty dates spanning the spring, summer

and autumn months. Total phytoplankton biomass throughout the seasons is presented in Fig. 3d and shows highest biomass in summer. A spring bloom in May comprised diatoms and *Phaeocystis*. In terms of biomass, the phytoplankton were dominated by dinoflagellates throughout the summer and into the autumn (Fig. 3d).

GBT seasonality

Samples of seawater particulates for GBT analysis were collected weekly (weather permitting) between March and December 2016, from Station L4 (Fig. 1). Clear seasonality in particulate GBT (Fig. 3f) was observed. GBT was detected in all particulate samples at concentrations ranging from 2 to 73 nmol L⁻¹ (Fig. 3f). Highest GBT concentrations were detected in summer and autumn (Fig. 3f) and show two distinct maxima of 68 and 73 nmol L⁻¹ in July

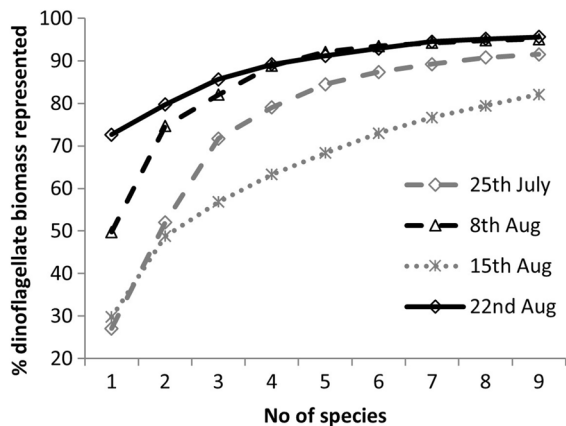


Fig. 3 Physicochemical properties, phytoplankton and particulate GBT concentrations in surface waters at Station L4 in 2016. **a** Chlorophyll *a* concentration (mg m^{-3}); **b** Sea surface temperature (SST, $^{\circ}\text{C}$) and surface salinity (PSU) data; **c** Nitrate and nitrite concentration (μM); **d** Total phytoplankton biomass (mg C m^{-3}); **e** Total dinoflagellate biomass (mg C m^{-3}); **f** Particulate GBT (nmol/L). Error bars represent standard deviation, $n=3$; Vertical dashed lines split the year seasonally where spring is March–May, summer is June–August and autumn is September–November

and September, respectively. The only other measurements of GBT at a coastal site were taken in the Gulf of Maine in June 1995, and fell in the range 0–15 nM, measured by HPLC (Keller et al. 2004). To investigate trends in the dataset further with PRIMER (Plymouth Routines In Multivariate Ecological Research, version 7.0.11; Primer-E Ltd.), a global BEST test was used to determine which L4 environmental variables best explained the variations in GBT concentration (further information on the PRIMER BEST test can be found in Clarke et al. 2008). Particulate GBT concentrations were divided into seasons (date of sample collection where spring is March–May, summer is June–August and autumn is September–November), transformed (overall square root, to reduce the influence of outliers) and normalised (to convert all the variables to a common dimensionless scale so that they can be combined in the analysis). The BEST test then statistically permutes the data and compares it to the actual trend observed. The results suggest that the particulate GBT concentrations observed at L4 are significant compared to 999 other random permutations of the data in every season tested. Following this, the BEST test uses the environmental variables (referred to as

the ‘explanatory matrix’ in Clarke et al. 2008) and the L4 GBT dataset (the ‘fixed resemblance matrix’) and calculates resemblance matrices to highlight whether any particular variable, or combination of variables, correlates with the GBT concentrations observed. The BEST test generates a list of highest ranked correlations between the fixed and explanatory matrices which exceed the value of those correlations occurring by chance. The BEST test highlighted that counts of dinoflagellates and *Phaeocystis*, together, best explained the particulate GBT seasonality with a correlation of 0.842, with the presence of dinoflagellates and the absence of *Phaeocystis* correlating with GBT concentration. Supplementary Fig. 1, adapted from non-metric Multi-Dimensional Scaling (nMDS) analyses in PRIMER following the BEST test, shows an absence of Particulate GBT (after normalisation; blue wedges) when *Phaeocystis* is present (green wedges) and the suggested link between GBT concentrations and dinoflagellates (red wedges). Labels with no coloured wedges indicate an absence of all three variables (GBT, *Phaeocystis* and dinoflagellates) after normalisation. This correlation supports previous culture experiments where dinoflagellates have been shown to markedly increase their cellular GBT content in response to increasing salinity, while maintaining a constant cell volume and DMSP content (Gebser and Pohnert 2013), but a link between dinoflagellates and GBT in the natural marine environment has not been demonstrated previously.

The measurements of GBT at L4 (Fig. 3f) show considerable variability in the magnitude of the relative standard deviation (Fig. 3f), particularly between summer sampling dates. The analytical method itself demonstrates excellent reproducibility, with precision for GBT of 3% (Beale and Airs 2016). During the summer period, the dinoflagellate species composition changed frequently; both in terms of the dominant dinoflagellate species, and the number of species contributing to the overall biomass (Table 3). The high relative standard deviation observed on 25th July and 15th August corresponded to a higher number of species contributing to the dinoflagellate biomass (Table 3; Fig. 4). Different dinoflagellate species are likely to differ in their susceptibility to breakage during filtering, due to their diverse morphological characteristics including cell size and armoured/unarmoured cells (Goldman and Dennet 1985). Several of the

Table 3 GBT concentration, phytoplankton and dinoflagellate biomass, and dinoflagellate composition during 4 consecutive weeks in summer 2016. ^L denotes cells $\geq 100 \mu\text{m}$ (see text).

Species above the bold line contribute to 75% of the dinoflagellate biomass for that sampling day. Species common to the four sampling points shown in this table are colour coded

Date	25 th July	8 th August	15 th August	22 nd August
GBT (sd) nmol L ⁻¹	68 (33)	43 (6)	44 (53)	15 (5.5)
Total phytoplankton biomass, mg C m ⁻³	210.0	89.1	53.0	113.5
Dinoflagellate biomass, mg C m ⁻³ (% of total)	194.5 (93%)	77.3 (87%)	37.7 (71%)	102.8 (91%)
Top 9 dinoflagellate species, (biomass; mg C m ⁻³)	<i>Scrippsiella</i> spp. (52.6)	<i>Karenia mikimotoi</i> (38.4)	<i>Ceratium lineatum</i> ^L (11.2)	<i>Karenia mikimotoi</i> (74.7)
	<i>Karenia mikimotoi</i> (48.4)	<i>Ceratium lineatum</i> ^L (19.3)	<i>Karenia mikimotoi</i> (7.2)	<i>Ceratium furca</i> ^L (7.3)
	<i>Dinophysis acuta</i> ^L (38.5)	<i>Gyrodinium spirale</i> (5.7)	<i>Dinophysis acuta</i> ^L (3.0)	<i>Dinophysis acuta</i> ^L (6.1)
	<i>Ceratium lineatum</i> ^L (14.2)	<i>Dinophysis acuta</i> ^L (5.3)	<i>Polykrikos schwartzii</i> ^L (2.4)	<i>Ceratium lineatum</i> ^L (3.6)
	<i>Gyrodinium</i> (large) (10.70)	<i>Gyrodinium</i> (large) (2.5)	<i>Gyrodinium</i> (medium) (1.9)	<i>Protoperidinium depressum</i> ^L (2.1)
	<i>Prorocentrum micans</i> (5.6)	<i>Gyrodinium</i> (medium) (1.1)	<i>Protoperidinium ovatum</i> (1.8)	<i>Protoperidinium ovatum</i> (1.8)
	<i>Gyrodinium</i> (medium) (5.1)	<i>Dinophysis tripos</i> (0.6)	<i>Noctiluca scintillans</i> ^L (1.4)	<i>Polykrikos schwartzii</i> ^L (1.6)
	<i>Dinophysis acuminata</i> (3.5)	<i>Prorocentrum micans</i> (0.5)	<i>Protoperidinium oceanicum</i> ^L (1.0)	<i>Gyrodinium</i> (medium) (0.7)
	<i>Protoperidinium depressum</i> ^L (3.1)	<i>Gyrodinium</i> (small) (0.2)	<i>Ceratium horridum</i> ^L (1.0)	<i>Ceratium horridum</i> ^L (0.5)

dinoflagellate species present comprised large cells ($\geq 100 \mu\text{m}$; Table 3). Very large cells can be difficult to sample reproducibly and the uneven distribution of large cells between samples can have a more pronounced effect on concentration differences between samples. The combination of the dinoflagellate biomass comprising a high diversity of species, and several of those species having large cell sizes, is likely to add variability to the sampling and therefore impact the relative standard deviations of

the concentrations observed. Increasing the sample volume could normally be an approach to decrease the observed variability but was not a viable solution here due to the loss of osmolytes observed with increased sample volume (Kiene and Slezak 2006). Increasing the number of replicates of samples could be a viable strategy, however.

The weekly dinoflagellate species composition during summer, measured by light microscopy, coupled with the seasonal GBT profile, enabled the

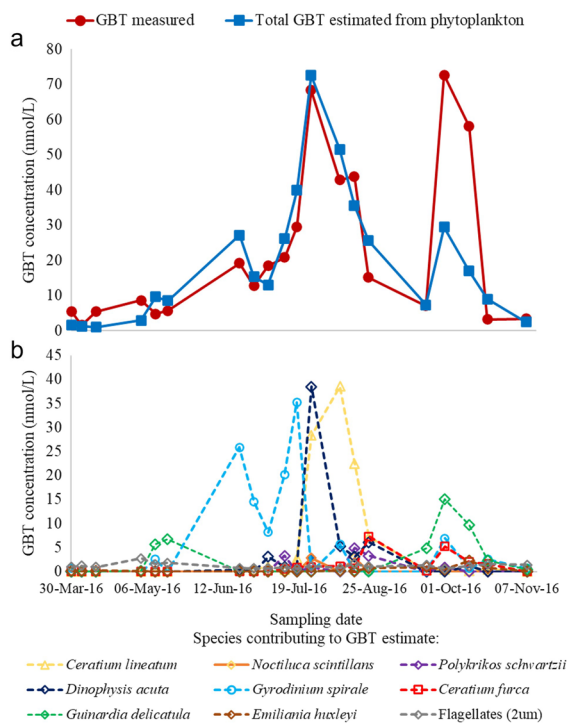


Fig. 4 Number of species contributing to the dinoflagellate biomass at Station L4 on the 25th July, 8th, 15th, and 22nd August 2016

prediction of dinoflagellate species that are likely to be GBT producers. Further, allocation of cellular GBT content to phytoplankton species present, permitted partial recreation of the seasonal GBT profile (Fig. 5). Intracellular GBT concentrations were estimated for six dinoflagellate species, a diatom, prymnesiophyte and small (2 μm) flagellates (Table 4) based on culture studies (Keller et al. 1999a, b; Spielmeyer et al. 2011). Dinoflagellates/phytoplankton not included in Table 4, that were found to be present at L4 (e.g. see Table 3) were assumed to have a negligible intracellular concentration of GBT. This enabled the summer profile of GBT concentrations to be reasonably well reproduced (Fig. 5a). Although being a significant contributor to the summer phytoplankton biomass (Table 3), our study suggests that *Karenia mikimotoi* is not a significant producer of GBT, as a ten-fold increase in *Karenia* biomass from the 15th to 22nd August, coincided with a decrease in the overall GBT concentration from 44 to 15 nM (Table 3). Notably, *K. mikimotoi* was also not attributed as a major DMSP producer by Archer et al.

(2009) and is therefore likely to employ alternative cellular osmolytes. The combination of GBT concentration and phytoplankton data provides useful information to direct field studies and culturing experiments investigating GBT production.

The autumn peak in GBT concentration did not correspond clearly with any component of the phytoplankton community. There were species that peaked concurrently with the autumn GBT maxima i.e. the diatom *Guinardia delicatula*, the dinoflagellates *Ceratium furca* and *Gyrodinium spirale*, and the coccolithophore *Emiliana huxleyi* (Fig. 5b). However, estimated cellular concentrations of GBT for these species (Table 4), based on literature values for cultures (Keller et al. 1999a, b; Spielmeyer et al. 2011) only accounted for 40% of the measured GBT autumn maximum (Fig. 5a). It should be noted, however, that the estimated cellular values include significant uncertainty for the following reasons: Keller et al. (1999a) found that the cellular GBT content in three phytoplankton cultures varied during the growth curve of the cells, indicating that the physiological state of the cells at L4 may be a contributing factor to their GBT content. Also, of the limited species-specific information available in the literature, there is much uncertainty over the GBT content of different species: For example, the dinoflagellate *Prorocentrum minimum* was found not to contain GBT by Keller et al. (1999a), but Spielmeyer et al. (2011) reported this species to be the highest GBT producer ($6.96 \text{ pg cell}^{-1}$) of those investigated. Furthermore, some of the studies on cultures relied on filtering relatively large volumes of sample (e.g. 50–700 mL) which may then have resulted in underestimations of the cellular measurements (Kiene and Slezak 2006). However, the overall phytoplankton biomass during the autumn period was low (Fig. 3), particularly compared to the summer period, indicating there were likely other sources of GBT in autumn. The osmolyte content of natural assemblages of zooplankton have been reported to be species-specific for the osmolyte DMSP (Tang et al. 2000) and can contribute substantially to particulate concentrations in the water column when these species are in high abundance (Tang et al. 2000). It made sense therefore to interrogate the zooplankton data from L4 for possible contributors to the GBT pool. Harpacticoid copepods were found to peak in biomass (up to 380 g C m^{-3}) coincident with the autumn GBT maxima. Although the water

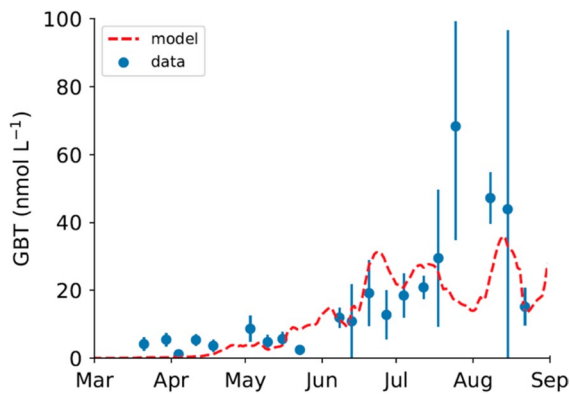


Fig. 5 **a** Particulate GBT concentrations at Station L4 measured (solid red line) and estimated (solid blue line) by assigning cellular concentrations to phytoplankton species present at L4. **b** The contribution to the estimated GBT concentration from individual phytoplankton species (see key)

samples for GBT analysis were screened through 200 μm mesh, the Harpacticoid copepods exhibit a broad range of sizes from first nauplii to adults of 35–>850 μm (Boxshall 1979), so smaller animals or body parts could have contributed to the GBT signal observed. Further, faeces from zooplankton present in the water sample could also have added to the GBT concentrations (de Angelis and Lee 1994). Some marine bacteria are known to use GBT (Lidbury et al.

Table 4 Assigned cellular concentration of GBT in phytoplankton species at Station L4 in summer (estimated from Keller et al. 1999a, b; Spielmeyer et al. 2011), used to reproduce measured concentrations of GBT in particulates

Phytoplankton species	Class	Assigned mmol GBT/L cell volume
<i>Ceratium lineatum</i>	Dinophyceae	244
<i>Noctiluca scintillans</i>	Dinophyceae	190
<i>Polykrikos schwartzii</i>	Dinophyceae	205
<i>Dinophysis acuta</i>	Dinophyceae	110
<i>Gyrodinium spirale</i>	Dinophyceae	104
<i>Ceratium furca</i>	Dinophyceae	114
<i>Guinardia delicatula</i>	Bacillariophyceae	221
<i>Emiliania huxleyi</i>	Prymnesiophyceae	167
Flagellates (2 μm)	–	198

2015; Noell et al. 2019), and GBT transporters are widespread in bacteria (McParland et al. 2021); bacteria are therefore likely to have contributed to the particulate GBT signal throughout the seasons. The proportion of the bacterial:phytoplankton contribution to the GBT concentration is unclear, however. It should also be noted that the autumn period of high GBT concentration coincided with an increase in salinity and nitrate concentration (Fig. 3); the salinity change may have prompted cells present to increase their osmolyte concentration, enabled by the increasing availability of inorganic N. Clearly, the summer and autumn maxima in GBT concentrations had different environmental drivers.

The significance of high GBT concentration in summer

The summer increase in GBT concentration concomitant with the lowest inorganic nutrient concentrations (Fig. 3) was intriguing and warranted further investigation. Elevated summer GBT concentrations aligned with increases in dinoflagellate biomass (Fig. 3). Specifically, the GBT data spanning from March to August 2016 may be clustered into two distinct groups depending on the season and the relative abundance of dinoflagellates (Table 2). In spring [Mar–Apr–May] GBT was always below 10 nmol L^{-1} and the dinoflagellate biomass did not exceed 40% of the total phytoplankton. In summer [June–July–August], GBT reached 66 nmol L^{-1} and the fraction of dinoflagellate biomass was consistently higher than 60% (> 90% in July). Further, in the summer period, inorganic nutrients (nitrate) were depleted (Fig. 3c). Starting from this evidence that summer GBT coincided with low inorganic nutrient concentrations, we therefore hypothesised that the observed summer GBT accumulation is related to nutrient stress (high C:N ratio; Supplementary Fig. 2) and that GBT has a positive feedback on dinoflagellate growth, giving them a competitive advantage in summer.

More specifically we propose that the high cellular content of quaternary ammonium derivatives such as glycine betaine positively affect the buoyancy of dinoflagellates as already suggested by Boyd and Gradmann (2002). Enhanced buoyancy aids dinoflagellates to (i) adjust their position in the water column to optimise light and nutrient

conditions and (ii) to match the depth of prey for mixotrophic species which are common and abundant within the dinoflagellate community at L4 (Gisselson et al. 2002; Tilstone et al. 2010).

While the synthesis of nitrogen containing metabolites under nutrient depleted conditions seems counterintuitive, literature evidence suggests that this is not uncommon in dinoflagellates. Dinoflagellates have been shown to survive under severe nutrient limiting conditions displaying very high carbon to nutrient molar ratios (C:N up to 20 and C:P up to 400; Pinna et al. 2015). The cellular content of nitrogen-containing chlorophyll is generally low in dinoflagellates (Geider et al. 1996, Polimene et al. 2014) suggesting that nitrogen can be allocated to different metabolites (e.g. osmolytes), better suited to support growth and fitness of this group under stressed conditions. For example, production of nutrient-containing secondary metabolites such as toxins have previously been associated with cellular nutrient deficiency (Van de Waal et al. 2014). Compatible solutes such as proline and GBT have already been proposed to accumulate under adverse environmental conditions, playing a wider role in stress tolerance besides osmoregulation (Hare et al. 1998).

Therefore, we used this hypothesis that summer GBT accumulation is related to nutrient stress and that GBT has a positive feedback on dinoflagellate growth as a concept to test via a modelling approach. We modified an established marine ecosystem model (ERSEM; Butenschön et al. 2016) by adding a new formulation describing enhanced GBT production by dinoflagellates as a function of nutrient stress. Additionally, in order to describe enhanced buoyancy as a function of GBT, we have assumed that intracellular GBT production reduces sinking. The positive effect of buoyancy on predation (for mixotrophic species) was challenging to simulate since mixotrophic behaviour is not modelled in ERSEM. However, we have indirectly simulated this effect by assuming that the cellular loss terms described in ERSEM decrease proportionally to the GBT to carbon ratio, in this way boosting net growth (i.e. gross production – loss terms, see Eqs. 2 and 4). Our formulation allowed the model to qualitatively reproduce both the increase in dinoflagellate biomass and GBT observed in the transition from spring to summer [Fig. 2; correlation coefficient R^2 between simulated and observed GBT

concentrations in spring-summer is 0.65 ($p < 0.005$)]. However, the highest GBT concentrations observed in summer are not fully captured by the model. This is not surprising given the strong model underestimation of biomass in summer (Table 2). Despite this, and in contrast to the standard ERSEM formulation, the new model manages to simulate the summer dominance of dinoflagellates (although only qualitatively) pushing the ERSEM simulation of this algal group towards realism (Table 2). The model thus corroborates our hypothesis that GBT promotes the growth and fitness of dinoflagellates in those ecosystems where inorganic nutrients are depleted (Fig. 3c) by earlier blooms. Additional field studies and laboratory experiments focussing on GBT production under different nutrient regimes are required to validate our hypothesis.

Conclusion

During three seasons in 2016, GBT concentrations varied from 3 to 73 nM at this temperate coastal site, which at times exceeds previous coastal measurements in the Gulf of Maine where GBT concentrations up to 15 nM were observed (Keller et al. 2004). However, the concentrations observed were lower than those typical for the osmolyte DMSP in the Western English Channel, which have been reported to reach 120 nM (Archer et al. 2009), a feature consistent with the more widespread distribution of DMSP than GBT in culture. Summer variation of particulate GBT concentrations at the coastal site L4 correlated with a dynamic population of dinoflagellates. We also suggest that, under nutrient deplete conditions, GBT production gives dinoflagellates a growth advantage allowing them to dominate the phytoplankton community in the summer months. Enhanced dinoflagellate growth could be due to the positive effects of quaternary amines on their buoyancy which could facilitate their vertical migration and access to nutrients in stratified water columns. Such a strategy would underpin a resilience to varying conditions under climate change scenarios. Such resilience in the face of climate change highlights a requirement for research into the impact and role of atmospheric methylamines in organic aerosol production. This process is proposed to be affected by the

release of N-osmolytes from phytoplankton cells, of which a significant contribution is likely to be from dinoflagellates.

Acknowledgements We thank Sarah Dashfield for assisting with sampling and the crew and support scientists on board the RV *Plymouth Quest* for their expertise on maintaining the Western Channel Observatory.

Author contributions YC and RLA conceived the study. RLA and RB planned and carried out the sampling, analysis and data interpretation of glycine betaine. CEW analysed phytoplankton by microscopy. GAT provided data from flow cytometry. AM provided zooplankton microscopy data. LP carried out ecosystem modelling. CH and EMSW analysed and provided nutrient data. RLA, RB, LP and CEW wrote the manuscript. All authors commented on and edited the manuscript.

Funding This research was supported by Natural Environment Research Council Grants NE/M00336/1, NE/P008526/1 and NE/M002233/1. Widdicombe, Tarran, Woodward and Harris were funded under the UK's National Environment Research Council's National Capability long-term Single Centre Science Programme, Climate Linked Atlantic Sector Science, CLASS, (NE/R015953/1), contribution to Theme 1.3 Biological Dynamics.

Data availability N-osmolyte data and model information are available from the British Oceanographic Data Centre, bodc.ac.uk/resources/inventories/edmed/report/7100/.

Code availability Model code is available via the British Oceanographic Data Centre (link above) and via <https://doi.org/10.5281/zenodo.4288840>.

Declarations

Conflict of interest No conflicts of interest.

Ethical approval Not applicable.

Consent to participate Not applicable.

Consent for publication All authors give consent for publication.

Open Access This article is licensed under a Creative Commons Attribution 4.0 International License, which permits use, sharing, adaptation, distribution and reproduction in any medium or format, as long as you give appropriate credit to the original author(s) and the source, provide a link to the Creative Commons licence, and indicate if changes were made. The images or other third party material in this article are included in the article's Creative Commons licence, unless indicated otherwise in a credit line to the material. If material is not included in the article's Creative Commons licence and your intended use is not permitted by statutory regulation or exceeds the permitted use, you will need to obtain permission directly

from the copyright holder. To view a copy of this licence, visit <http://creativecommons.org/licenses/by/4.0/>.

References

- Airs RL, Archer SD (2010) Analysis of glycine betaine and choline in seawater particulates by liquid chromatography/electrospray ionization/mass spectrometry. *Limnol Oceanogr Methods* 8:499–506. <https://doi.org/10.4319/lom.2010.8.499>
- Almeida J, Schobesberger S, Kürten A et al (2013) Molecular understanding of sulphuric acid-amine particle nucleation in the atmosphere. *Nature* 502:359. <https://doi.org/10.1038/nature12663>
- Archer S, Cummings D, Llewellyn C, Fishwick J (2009) Phytoplankton taxa, irradiance and nutrient availability determine the seasonal cycle of DMSP in temperate shelf seas. *Mar Ecol Prog Ser* 394:111–124. <https://doi.org/10.3354/meps08284>
- Beale R, Airs R (2016) Quantification of glycine betaine, choline and trimethylamine *N*-oxide in seawater particulates: Minimisation of seawater associated ion suppression. *Anal Chim Acta* 938:14–122. <https://doi.org/10.1016/j.aca.2016.07.016>
- Boxshall GA (1979) The planktonic copepods of the northeastern Atlantic Ocean: Harpacticoida, Siphonostomatoida and Mormonilloida. *Bull Br Museum (Natural History)* 35:201–264
- Boyd C, Gradmann D (2002) Impact of osmolytes on buoyancy of marine phytoplankton. *Mar Biol* 141:605–618. <https://doi.org/10.1007/s00227-002-0872-z>
- Boysen AK, Heal KR, Carlson LT, Ingalls AE (2018) Best-matched internal standard normalization in liquid chromatography-mass spectrometry metabolomics applied to environmental samples. *Anal Chem* 90:1363–1369
- Boysen AK, Carlson LT, Durham BP, Groussman RD, Aylward FO, Ribalet F, Heal KR, White AE, DeLong EF, Armbrust EV, Ingalls AE (2021) Particulate metabolites and transcripts reflect diel oscillations of microbial activity in the surface ocean. *mSystems* 6:e00896–e00820. <https://doi.org/10.1128/mSystems.00896-20>
- Boysen AK, Durham BP, Kumler W, Key RS, Heal KR, Carlson LT, Groussman RD, Armbrust EV, Ingalls AE (2022) Glycine betaine uptake and metabolism in marine microbial communities. *Environ Microbiol* 24:2380–2240
- Burchard H, Bolding K, Villarreal M (1999) GOTM, a general ocean turbulence model. Theory, implementation and test cases. Technical Report EUR 18745 EN, European Commission
- Butenschön M, Clark J, Aldridge JN, Allen JI, Artioli Y, Blackford J, Bruggeman J, Cazenave P, Ciavatta S, Kay S, Lessin G, van Leeuwen S, van der Molen J, de Mora L, Polimene L, Saille S, Stephens S, Torres R (2016) ERSEM 15.06: a generic model for marine biogeochemistry and the ecosystem dynamics of the lower trophic levels. *Geosci Model Dev* 9:1293–1339. <https://doi.org/10.5194/gmd-9-1293-2016>
- Clarke KR, Somerfield PJ, Gorley RN (2008) Testing of null hypotheses in exploratory community analyses: similarity

- profiles and biota-environment linkage. *J Exp Mar Biol Ecol* 366:56–69
- Dall'Osto M, Ovadnevaite J, Paglione M, Beddows DCS, Ceburnis D, Cree C, Cortés P, Zamanillo M, Nunes SO, Pérez GL, Ortega-Retuerta E, Emelianov M, Vaqué D, Marrasé C, Estrada M, Montserrat Sala M, Vidal M, Fitzsimons MF, Beale R, Airs R, Rinaldi M, Decesari S, Faccini MC, Harrison RM, O'Dowd C, Simó R (2017) Antarctic sea ice region as a source of biogenic organic nitrogen in aerosols. *Sci Rep* 7:6047. <https://doi.org/10.1038/s41598-017-06188-x>
- Dall'Osto M, Airs RL, Beale R, Cree C, Fitzsimons M, Beddows D, Harrison RM, Ceburnis D, O'Dowd C, Rinaldi M, Paglione M, Nenes A, Decesari S, Simó R (2019) Simultaneous detection of alkylamines in the surface ocean and atmosphere of the Antarctic sympagic environment. *ACS Earth and Space Chemistry* 3:854–862. <https://doi.org/10.1021/acsearthspacechem.9b00028>
- de Angelis M, Lee C (1994) Methane production during zooplankton grazing on marine phytoplankton. *Limnol Oceanogr* 39:1298–1308
- Fuhrman J, Bell T (1985) Biological considerations in the measurement of dissolved free amino-acids in seawater and implications for chemical and microbiological studies. *Mar Ecol Prog Ser* 25:13–21
- Galí M, Devred E, Levasseur M, Royer S-J, Babin M (2015) A remote sensing algorithm for planktonic dimethylsulfoniopropionate (DMSP) and an analysis of global patterns. *Remote Sens Environ* 171:171–184. <https://doi.org/10.1016/j.rse.2015.10.012>
- Gebser B, Pohnert G (2013) Synchronized regulation of different zwitterionic metabolites in the osmoadaptation of phytoplankton. *Mar Drugs* 11:2168–2182. <https://doi.org/10.3390/md11062168>
- Geider R, MacIntyre H, Kana T (1996) A dynamic model of photoadaptation in phytoplankton. *Limnol Oceanogr* 41:1–15
- Gisselson L-A, Carlsson P, Granéli E, Pallon J (2002) *Dinophysis* blooms in the deep euphotic zone of the Baltic Sea: do they grow in the dark? *Harmful Algae* 1:401–418. [https://doi.org/10.1016/S1568-9883\(02\)00050-1](https://doi.org/10.1016/S1568-9883(02)00050-1)
- Goldman JC, Dennet MR (1985) Susceptibility of some marine phytoplankton species to cell breakage during filtration and post-filtration rinsing. *J Exp Mar Biol Ecol* 86:47–58. [https://doi.org/10.1016/0022-0981\(85\)90041-3](https://doi.org/10.1016/0022-0981(85)90041-3)
- Hare P, Cress W, Van Staden J (1998) Dissecting the roles of osmolyte accumulation during stress. *Plant Cell Environ* 21:535–553. <https://doi.org/10.1046/j.1365-3040.1998.00309.x>
- Heijthuisen J, Hansen T (1989) Betaine fermentation and oxidation by marine *Desulfuromonas* strains. *Appl Environ Microbiol* 55:965–969
- Johnson WM, Longnecker K, Kido Soule MC, Arnold WA, Bhatia MP, Hallam SJ, Van Mooy BAS, Kujawinski EB (2020) Metabolite composition of sinking particles differs from surface suspended particles across a latitudinal transect in the Southern Atlantic. *Limnol Oceanogr* 65:111–127. <https://doi.org/10.1002/lno.11255>
- Kageyama H, Tanaka Y, Takabe T (2018) Biosynthetic pathways of glycinebetaine in *Thalassiosira pseudonana* functional characterization of enzyme catalyzing three-step methylation of glycine. *Plant Physiol Bioch* 127:248–255. <https://doi.org/10.1016/j.plaphy.2018.03.032>
- Keller M, Kiene R, Matrai P, Bellows W (1999a) Production of glycine betaine and dimethylsulfoniopropionate in marine phytoplankton. I. Batch cultures. *Mar Biol* 135:237–248. <https://doi.org/10.1007/s002270050621>
- Keller M, Kiene R, Matrai P, Bellows W (1999b) Production of glycine betaine and dimethylsulfoniopropionate in marine phytoplankton. II. N-limited chemostat cultures. *Mar Biol* 135:249–257. <https://doi.org/10.1007/s002270050622>
- Keller M, Matrai P, Kiene R, Bellows W (2004) Responses of coastal phytoplankton populations to nitrogen additions: dynamics of cell-associated dimethylsulfoniopropionate (DMSP), glycine betaine (GBT), and homarine. *Can J Fish Aquat Sci* 61:685–699. <https://doi.org/10.1139/f04-058>
- Kiene R, Slezak D (2006) Low dissolved DMSP concentrations in seawater revealed by small volume gravity filtration and dialysis sampling. *Limnol Oceanogr Methods* 4:80–95. <https://doi.org/10.4319/lom.2006.4.80>
- King G (1984) Metabolism of trimethylamine, choline and glycine betaine by sulfate-reducing and methanogenic bacteria in marine sediments. *Appl Environ Microb* 48:719–725
- Kondo Y, Sakamoto A, Nonaka H, Hayashi H, Saradhi PP, Chen TH, Murata N N (1999) Enhanced tolerance to light stress of transgenic *Arabidopsis* plants that express the *codA* gene for a bacterial choline oxidase. *Plant Mol Biol* 40(2):279–288
- Lidbury I, Kimberley G, Scanlan D, Murrell J, Chen Y (2015) Comparative genomics and mutagenesis of choline metabolism in the marine *Roseobacter* clade. *Environ Microbiol* 17:5048–5062. <https://doi.org/10.1111/1462-2920.12943>
- Mausz MA, Airs RL, Dixon JL, Widdicombe CE, Tarran GA, Polimene L, Dashfield S, Beale R, Scanlan DJ, Chen Y (2022) Microbial uptake dynamics of choline and glycine betaine in coastal seawater. *Limnol Oceanogr* 9999:1–13
- McParland EL, Alexander H, Johnson WM (2021) The osmolyte ties that bind: genomic insights into synthesis and breakdown of organic osmolytes in marine microbes. *Front Mar Sci* 8:732
- Menden-Deuer S, Lessard E (2000) Carbon to volume relationships for dinoflagellates, diatoms, and other protist plankton. *Limnol Oceanogr* 45:569–579. <https://doi.org/10.4319/lo.2000.45.3.0569>
- Noell S, Giovannoni S (2019) SAR11 bacteria have a high affinity and multifunctional glycine betaine transporter. *Environ Microbiol* 21:2559–2575. <https://doi.org/10.1111/1462-2920.14649>
- Papageorgiou GC, Murata N (1995) The unusually strong stabilizing effects of glycine betaine on the structure and function of the oxygen-evolving photosystem-II complex. *Photosynth Res* 44:243–252. <https://doi.org/10.1007/BF00048597>
- Pinna A, Pezolesi L, Pistocchi R, Vanucci S, Ciavatta S, Polimene L (2015) Modelling the stoichiometric regulation of C-rich toxins in marine dinoflagellates. *PLoS ONE* 10:e0139046. <https://doi.org/10.1371/journal.pone.0139046>
- Prasad KVSK, Saradhi PP (2004) Enhanced tolerance to photoinhibition in transgenic plants through targeting of

- glycine betaine biosynthesis into the chloroplasts. *Plant Sci* 166:1197–1212. <https://doi.org/10.1016/j.plantsci.2003.12.031>
- Polimene L, Archer SD, Butenschön M, Allen JI (2012) A mechanistic explanation of the Sargasso Sea DMS “summer paradox”. *Biogeochemistry* 110:243–255
- Polimene L, Brunet C, Butenschön M, Martinez-Vicente V, Widdicombe C, Torres R, Allen J (2014) Modelling a light-driven phytoplankton succession. *J Plank Res* 36:214–229. <https://doi.org/10.1093/plankt/fbt086>
- PRIMER Plymouth Routines In Multivariate Ecological Research, version 7.0.11; Primer-E Ltd
- Riccobono F, Schobesberger S, Scott CE et al (2014) Oxidation products of biogenic emissions contribute to nucleation of atmospheric particles. *Science* 344:717. <https://doi.org/10.1126/science.1243527>
- Sacks JS, Heal KR, Boysen AK, Carlson LT, Ingalls AE (2022) Quantification of dissolved metabolites in environmental samples through cation-exchange solid-phase extraction paired with liquid chromatography-mass spectrometry. *Limnol Oceanogr : Methods*. <https://doi.org/10.1002/lom3.10513>
- Seymour J, Simó R, Ahmed T, Stocker R (2010) Chemoattraction to dimethylsulfoniopropionate throughout the marine microbial food web. *Science* 329:342–345. <https://doi.org/10.1126/science.1188418>
- Smyth T, Fishwick J, Ali-Moosawi L, Cummings D, Harris C, Kitidis V, Rees A, Martinez-Vicente V, Woodward E (2010) A broad spatio-temporal view of the western English Channel observatory. *J Plankton Res* 32:585–601. <https://doi.org/10.1093/plankt/fbp128>
- Spielmeier A, Gebser B, Pohnert G (2011) Dimethyl sulphide sources from microalgae: improvement and application of a derivatization-based method for the determination of dimethylsulfoniopropionate and other zwitterionic osmolytes in phytoplankton. *Mar Chem* 124:48–56. <https://doi.org/10.1016/j.marchem.2010.12.001>
- Tang KW, Rogers DR, Dam HG, Visscher PT (2000) Seasonal distribution of DMSP among seston, dissolved matter and zooplankton along a transect in the Long Island Sound Estuary. *Mar Ecol Prog Ser* 206:1–11
- Thomas D, Dieckmann G (2002) Antarctic sea ice—a habitat for extremophiles. *Science* 295:641–644. <https://doi.org/10.1126/science.1063391>
- Tilstone G, Airs R, Martinez-Vicente V, Widdicombe C, Llewellyn C (2010) High concentrations of mycosporine-like amino acids and colored dissolved organic matter in the sea surface microlayer off the Iberian Peninsula. *Limnol Oceanogr* 55:1835–1850. <https://doi.org/10.4319/lo.2010.55.5.1835>.)
- Torres R, Artoli Y, Kitidis V, Ciavatta S, Ruiz-Villarreal M, Shutler J, Polimene L, Martinez V, Widdicombe C, Woodward EMS, Smyth T, Fishwick J (2020) Sensitivity of modelled CO₂ air-sea flux in a coastal environment to surface temperature, gradients, surfactants and satellite data assimilation. *Remote Sensing* 12:2038
- Van de Waal D, Smith V, Declerck S, Stam E, Elser J (2014) Stoichiometric regulation of phytoplankton toxins. *Ecol Lett* 17:736–742. <https://doi.org/10.1111/ele.12280>
- Watkins A, Roussel E, Parkes R, Sass H (2014) Glycine betaine as a direct substrate for methanogens (*Methanococoides* spp.). *Appl Environ Microb* 80:289–293. <https://doi.org/10.1128/AEM.03076-13>
- Welschmeyer NA (1994) Fluorometric analysis of chlorophyll *a* in the presence of chlorophyll *b* and pheopigments. *Limnol Oceanogr* 39:1985–1992
- Widdicombe C, Eloire D, Harbour D, Harris R, Somerfield P (2010) Long-term phytoplankton community dynamics in the western English Channel. *J Plankton Res* 32:643–655. <https://doi.org/10.1093/plankt/fbp127>
- Woodward E, Rees A (2001) Nutrient distributions in an anti-cyclonic eddy in the northeast Atlantic Ocean, with reference to nanomolar ammonium concentrations. *Deep Sea Res II* 48:775–793. [https://doi.org/10.1016/S0967-0645\(00\)00097-7](https://doi.org/10.1016/S0967-0645(00)00097-7)
- Yancey P (2005) Organic osmolytes as compatible, metabolic and counteracting cytoprotectants in high osmolarity and other stresses. *J Exp Biol* 208:2819–2830. <https://doi.org/10.1242/jeb.01730>
- Zecher K, Hayes KR, Philipp B (2020) Evidence of interdomain ammonium cross-feeding from methylamine- and glycine betaine-degrading Rhodobacteraceae to diatoms as a widespread interaction in the marine picosphere. *Front Microbiol* 11:53389. <https://doi.org/10.53389/fmicb.52020.533894>

Publisher's Note Springer Nature remains neutral with regard to jurisdictional claims in published maps and institutional affiliations.